Title
Seismic-velocity inversion using surface-wave tomography

Authors
Wu, Zheshu
Rector, James

Publication Date
2018-08-27

DOI
10.1190/segam2018-2998108.1

Peer reviewed

Seismic velocity inversion using surface wave tomography

Zheshu Wu
*
, Tsinghua University, University of California, Berkeley and James Rector, University of California, Berkeley

Seismic velocity inversion using surface wave tomography
Zheshu Wu
*
, Tsinghua University, University of California,

Berkeley and James Rector, University of California, Berkeley

Seismic velocity inversion using surface wave tomography

Zheshu Wu
*
, Tsinghua University, University of California, Berkeley and James Rector, University of California, Berkeley

Zheshu Wu
*
, Tsinghua University, University of California, Berkeley and James Rector, University of California, Berkeley

Zheshu Wu

*
, Tsinghua University,
University of California,
Berkeley and James Rector,
University of California,
Berkeley
Zheshu Wu
*
, Tsinghua University,
University of California,
Berkeley and James Rector,
University of California,
Berkeley
UMMARY
In this paper, we present the workflow of the application of surface wave tomography to characterize the near surface. A

near surface model is simulated with a shallow unconsolidated layer that has a variable thickness and a deep consolidated zone. Data is filtered by bandpass filters and surface wave phase arrival times are picked, and surface wave velocities are inverted using a ray theoretical tomographic approach. A good agreement is found between the inverted results and the original model. In another model, a thin fault zone is detected. Agreement between the tomographic results and the model suggests that surface wave tomography is well suited for characterizing

shallow geology with the capability of identifying low velocity anomalies and general lateral variations

Zheshu Wu∗, *Tsinghua University, University of California, Berkeley* and James Rector, *University of California, Berkeley*

SUMMARY

In this paper, we present the workflow of the application of surface wave tomography to characterize the near surface. A near surface model is simulated with a shallow unconsolidated layer that has a variable thickness and a deep consolidated zone. Data is filtered by bandpass filters and surface wave phase arrival times are picked, and surface wave velocities are inverted using a ray theoretical tomographic approach. A good agreement is found between the inverted results and the original model. In another model, a thin fault zone is detected. Agreement between the tomographic results and the model suggests that surface wave tomography is well suited for characterizing shallow geology with the capability of identifying low velocity anomalies and general lateral variations.

INTRODUCTION

Tomography technique has been a research topic of interest in geophysics for decades. Tomography is essentially an image reconstruction technique from projections (Herman, 2009). For seismic data, there are typically two kinds of tomography techniques: reflection tomography and transmission tomography (Bording et al., 1987).

The use of surface waves for tomography was widely adopted to invert for regional velocity fields using earthquake sources. Some representative works of this topic include Ritzwoller and Levshin (1998), Shapiro et al. (2005), Sabra et al. (2005) and so on. However, the use of surface waves for exploration or shallow site studies was limited to 2-D techniques like MASW (Park et al., 1999). Recently it has been shown that surface wave tomography using active sources in a prescribed geometry is well suited for shear velocity inversion in a local area. Sherman et al. (2014) represented a result of detecting tunnels using surface wave based methods including

attenuation tomography. Rector et al. (2015) and Alyousuf et al. (2017) applied surface wave tomographic imaging method to characterizing shallow areas.

In this paper, we present a workflow for surface wave tomography and compare it against a known model. A near surface model is simulated using an elastic finite difference wave equation code (Petersson and Sjögreen, 2017). Data is collected and filtered by a series of bandpass filters and surface wave phase arrival times are picked. The traveltime inversion is solved using singular value decomposition (SVD) approach. The inverted results are analyzed compared with the known model. A model with fault included is also performed. The inverted results from synthetic data suggest that surface wave tomography is well suited for characterizing shallow area with the capability of identifying low velocity anomalies and general lateral variations. However, the results also demonstrate that lateral and vertical resolution is limited by the wavelength of the data (Williamson and Worthington, 1993).

THEORY

The essence of travel time tomography is the fact that the travel time associated with a given ray (i.e. the total transmit time from source to receiver) is the integrated slowness along that raypath (Bording et al., 1987). In two-dimensional case, we have

$$t(ray) = \int_{ray} s(x,z)dl \qquad (1)$$

where x and z are horizontal and vertical coordinates, dl is the differential distance along the ray, $s(x, z)$ is the slowness (reciprocal velocity) at the point (x, z). It's common to discretize the model by square cells of constant size, within which the slowness is regarded as constant (Stewart, 1991). Then the inversion problem of the discretized model becomes

$$t = \sum_{i=1}^{n} d_i \cdot s_i \qquad (2)$$

where t is the travel time of the ray from source to receiver, di is the raypath length within the ith cell, s_i is the slowness of the ith cell, and n is the total number of cells traversed by the raypath. Since in a typical survey we get hundreds of raypaths and the same amount of traveltimes consequently, Equation (2) becomes a set of linear equations, which can be expressed in the following form

$$[t] = [D][s] \qquad (3)$$

where [t] is the traveltime vector, [D] is the matrix of raypath length in corresponding pixels, and [s] is the slowness vector sorted in a certain order which is the vector of unknowns we want to invert for.

MINING BENCH MODEL

The model is 220 m along x direction and 108 m along y direction. The free surface is a step-shaped mining site, with the platform surrounded by slopes, which is illustrated in Figure 1. We assume a two layer formation in this area. The first layer is a weathered layer, with average v_p from 400 m/s at surface to 1200 m/s at depth of around 5m. The second layer is less weathered, with average velocity of 2500 m/s.

The interface between these two layers is not flat but has some variations in depth, as shown in Figure 2. Both layers have 5% randomness for velocity, which is added to approximate the complexity of a real heterogeneous earth. The computation domain is surrouded by absorbing boundaries.

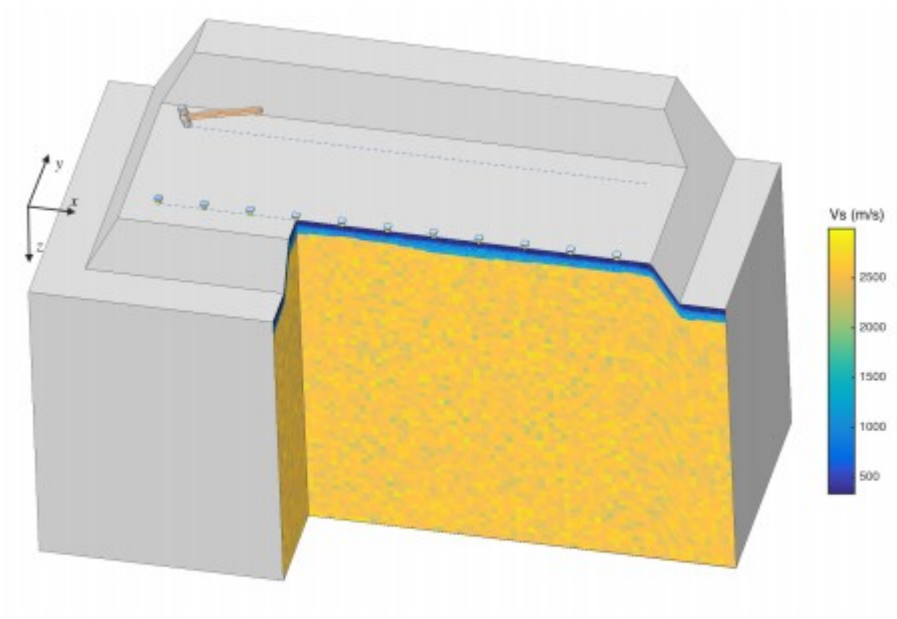

Figure 1: Mining bench model and the positions of source and receiver lines

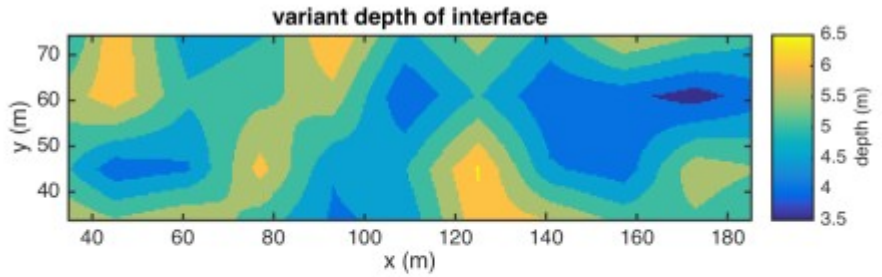

Figure 2: Depth variation of the interface between the weathered layered and the less weathered layer below it

The sources and receivers are all located on the platform of z = 0m. The sources are applied in a line with spacing of 3m, starting at (35, 74)m on the left end (where the sledgehammer is placed). The receiver line is parallel to the source line 40m away, also with a 3m spacing. A total of 51 shots are modeled (but for clarification there are only 11 receivers plotted here).

A 4th-order finite difference wave equation program SW4 (Petersson and Sjögreen, 2017) is used to simulate the wave progagation and synthetic data is collected. One representative shot gather data is shown in Figure 3.

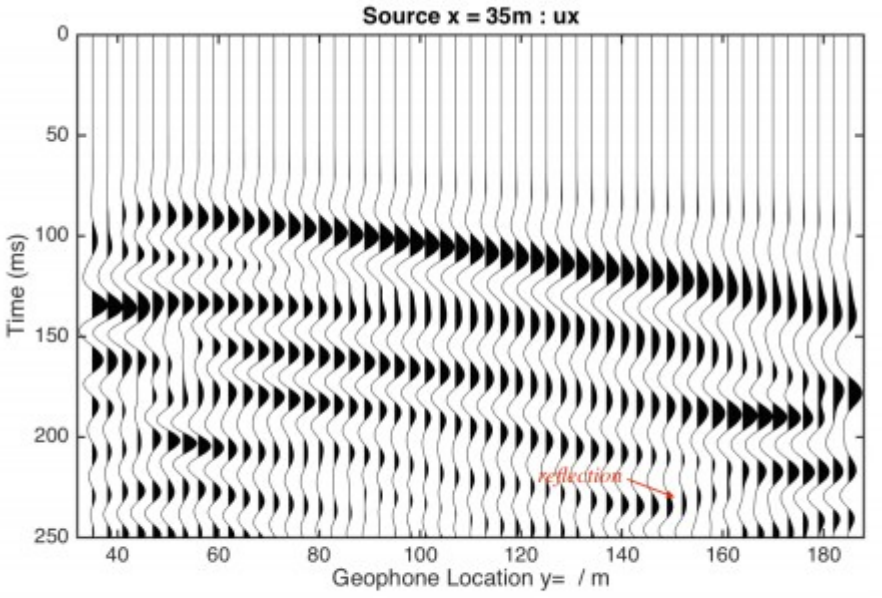

Figure 3: The shot gather of source at x = 35m

Surface waves are identified from the figure characterizing higher amplitudes but lower frequencies. Some reflections from the bench

boundaries, especially from the right boundary as pointed in the data, are detected as well.

Data processing

We applied bandpass filters at different frequencies ranging from 15 Hz to 75 Hz, each with a 5 Hz-wide bandpass window. Constant phase arrival times are picked for different frequencies. The arrival times are picked with 2-D calibration data as reference. The filtered data of 25 Hz center frequency is shown in Figure 4.

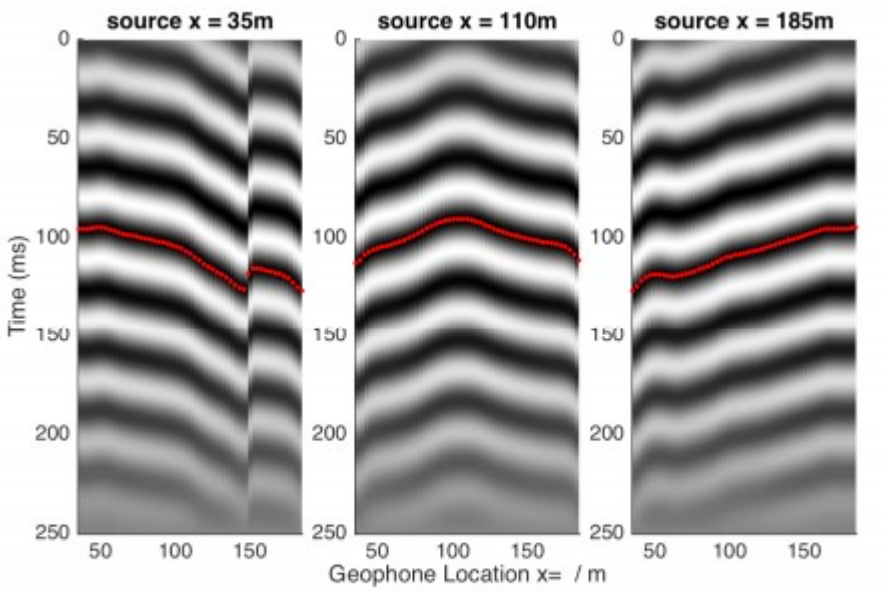

Figure 4: Shot gathers of source on the left, in the middle and on the right with center frequency of 25 Hz

Seismic inversion by SVD

Due to a large number of traces obtained and the limited geometry in surface wave survey, Equation 3 is usually overdetermined and the distance matrix [D] is ill-posed. Thus, a least-square solution is sought which minimizes the misfit of the traveltimes.

Among techniques to get the least-square solution of Equation 3, the singular value decomposition (SVD) method is often the most numerically robust (Lawson and Hanson, 1974; Lines and Treitel, 1984), where the solution is expanded as a weighted sum of parameter eigenvectors with weights in terms of the singular value λ_i. To avoid the adverse effect of too small singular value λ_i on the solution, Marquardst's damping factor β is usually

included in SVD (Lines and Treitel, 1984), which makes the weights become $\frac{\lambda_i}{\lambda_i^2+\beta}$, by which division by zero is obviously avoided even if λ_i approaches 0.

The damping factor is effectively a regularization in general least-square solutions, but it also makes the regularized solution strongly dependent on the parameter. Song and Zhang (1999) proposed a modified SVD solution where β is replaced by α_i which linearly increases with the index i as one implementation. This modified solution makes use of the properties of SVD that high (low) frequencies are associated with singular vectors corresponding to small (large) singular values, and somehow eliminates the difficulty in parameter choosing. Figure 5 shows the effect of different initial values α_0 on the weights. It can be seen that α_0 tends to impact the weight of singular vector corresponding to small singular value more than that of larger singular values, which means larger α_0 leads to more smoothing to the final inverted results. Here $\alpha_0 = 0.05$ is selected.

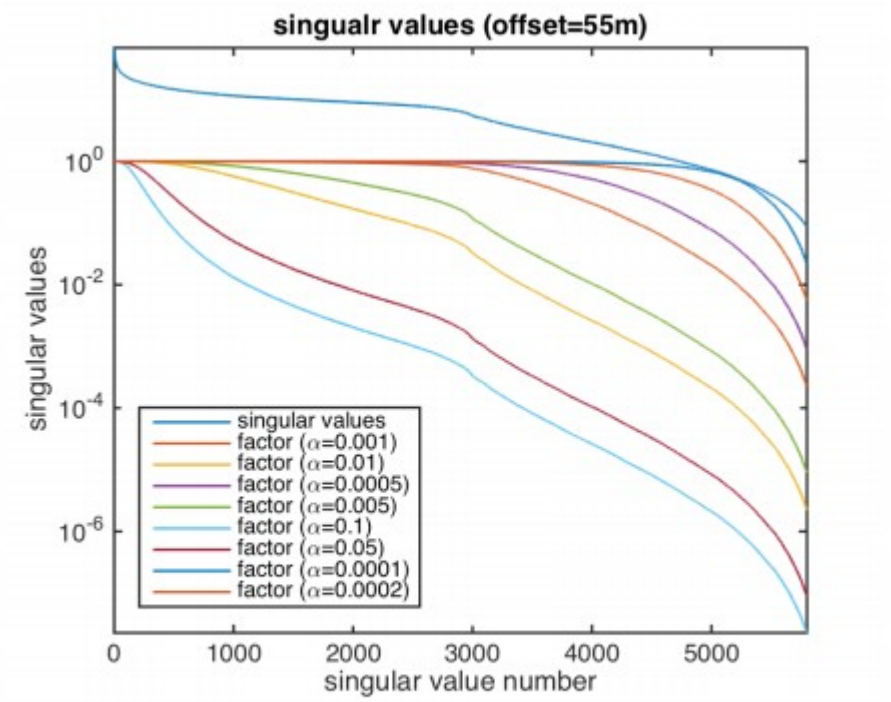

Figure 5: The effect of different initial values α_0 on the weights

Results

The inverted velocity field using a bandpass filter with center frequency of 25 Hz is shown in Figure 6. This relatively lower frequency results in a longer wavelength, therefore penetrating deeper into the lower unweathered layer.

The average velocity inverted is about 2100 m/s, compared to the model, 2500 m/s. The lateral variation is a little bit similar to the depth variation of the interface, reflecting the effect of the interface.

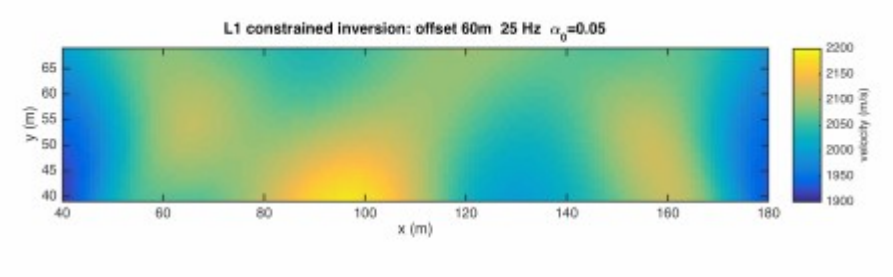

Figure 6: Tomogram at frequency of 25 Hz

Surface wave with higher frequencies have relatively shorter wavelength, thus propagating nearer to the surface. Figure 7 is the inverted phase velocity field at frequency of 72 Hz. It can be seen that there is more lateral variation at this frequency range. The pattern of the lateral variation conforms to some extent to the patter of the depth variation of the interface, which leads to the variation of the vertical averaged velocity.

It is noted that the average velocity inverted at high frequency as 72 Hz is around 1400 m/s, which is larger than the average velocity, less than 1000 m/s, of the first layer. Even higher frequency is needed to invert for the velocities above a much shallower area, but strong scattering and noise make it too hard to pick the accurate surface wave arrival time in this high frequency range, compromising the capability of surface wave tomography.

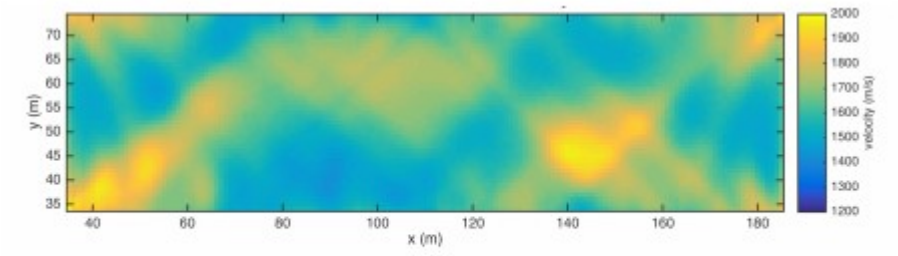

Figure 7: Inverted phase velocity field at frequency of 72 Hz

Fault model

Here we add an effect of low velocity fault into the model, in a hope to verify the capability of surface wave tomography to image fault zones. This can be useful in mining applications and geotechnical studies.

The fault is oriented 45◦ counterclockwise against the positive x direction with thickness of 1m, extending to the bottom of the model with a dipping angle of 60◦ . Figure 8a shows the vertically-averaged velocity of each pixel from surface to 20 m deep. Figure 8b is the inverted velocity field from the phase arrival times of 25 Hz center frequency.

Compared with the inverted result of the model without a fault, it is obvious that a low velocity area appears near $x = 118 \sim 158$ m, and is roughly oriented 40◦ against positive x. Although the shape of the low velocity is not exactly identical to the fault in the model and dependent on the parameters of the SVD solution, a low velocity anomaly can be roughly identified for further investigation through surface wave tomography.

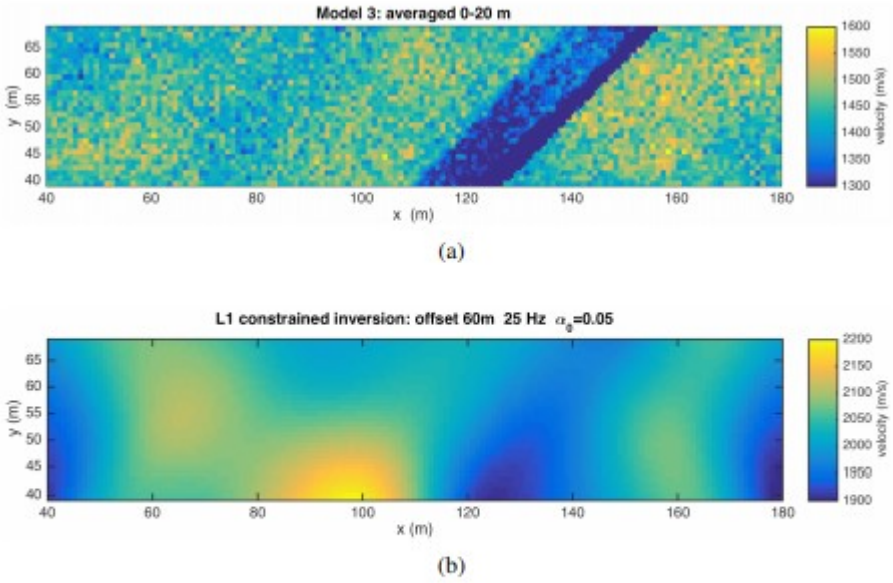

Figure 8: Comparison of the inverted result and the averaged velocity field of the original model

In addition, from the common offset gather (Figure 9) whose traces are oriented parallel to the fault inclination, we can clearly identify guided wave from the trace whose raypath is nearly along the fault. The guided wave has a distinct signature associated with trapped waves inside the low velocity fault zone.

CONCLUSIONS

From the above investigation of a numerical experiment, it is found that surface wave tomography is well suited for characterizing shallow areas.

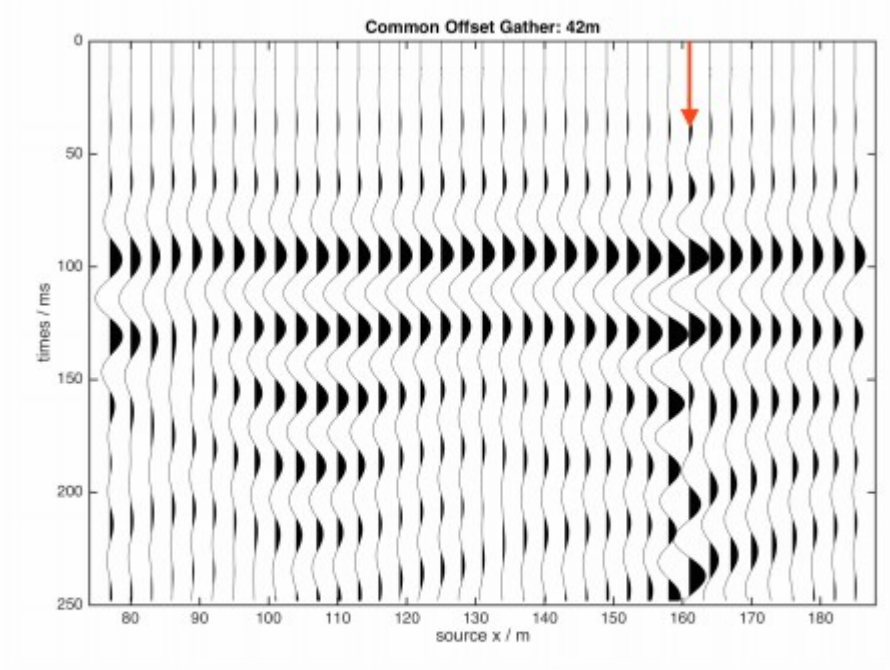

Figure 9: Common offset gather of offset=42m. The guided wave is marked with an arrow.

But there are significant lateral and vertical resolution limitations of surface wave traveltime tomography which compromises its wide application in near surface survey. Further work on developing better tomographic methods needs to be done to make surface wave tomography more applicable and more robust.

Acknowledgments

We would like to thank Bob Basker for his great help in processing the data. Zheshu Wu acknowledges China Scholarship Council for its financial support for his research at UC Berkeley.

REFERENCES

Alyousuf, T., J. Rector, G. Newman, and P. Petrov, 2017, Surface-wave tomography to resolve water table: Almond orchard case study, modesto, california: 87th Annual International Meeting, SEG, Expanded Abstracts, https://doi.org/10.1190/segam2017-17588536.1.

Bording, R. P., A. Gersztenkorn, L. R. Lines, J. A. Scales, and S. Treitel, 1987, Applications of seismic travel-time tomography: Geophysical Journal International, 90, 285–303, https://doi.org/10.1111/j.1365-246X.1987.tb00728.x.

Herman, G. T., 2009, Fundamentals of computerized tomography: Image reconstruction from projections: Springer Science and Business Media.

Lawson, C., and R. Hanson, 1974, Solving least squares problems: SIAM.

Lines, L., and S. Treitel, 1984, Tutorial: A review of least-squares inversion and its application to geophysical problems: Geophysical prospecting, 32, 159–186, https://doi.org/10.1111/j.1365-2478.1984.tb00726.x.

Park, C. B., R. D. Miller, and J. Xia, 1999, Multichannel analysis of surface waves: Geophysics, 64, 800–808, https://doi.org/10.1190/1.1444590.

Petersson, N. A., and B. Sjögreen, 2017, User's guide to sw4, version 2.0: Technical report, Lawrence Livermore National Laboratory, Livermore, CA.

Rector, J., J. Pfeiffe, S. Hodges, J. Kingman, and E. Sprott, 2015, Tomographic imaging of surface waves: A case study from the phoenix mine, battle mountain, nevada: The Leading Edge, 34, 1360–1364, https://doi.org/10.1190/tle34111360.1.

Ritzwoller, M. H., and A. L. Levshin, 1998, Eurasian surface wave tomography: Group velocities: Journal of Geophysical Research: Solid Earth, 103, 4839–4878, https://doi.org/10.1029/97JB02622.

Sabra, K. G., P. Gerstoft, P. Roux, W. Kuperman, and M. C. Fehler, 2005, Surface wave tomography from microseisms in southern California: Geophysical Research Letters, 32, https://doi.org/10.1029/2005GL023155.

Shapiro, N. M., M. Campillo, L. Stehly, and M. H. Ritzwoller, 2005, High-resolution surface-wave tomography from ambient seismic noise: Science, 307, 1615–1618, https://doi.org/10.1126/science.1108339.

Sherman, C., J. Rector, D. Dreger, and S. Glaser, 2014, Seismic tunnel detection at black diamond mines regional preserve: 84th Annual International Meeting, SEG, Expanded Abstracts, https://doi.org/10.1190/segam2014-1591.1.

Song, L.-P., and S.-Y. Zhang, 1999, Singular value decomposition-based reconstruction algorithm for seismic traveltime tomography: IEEE Transactions on Image Processing, 8, 1152–1154, https://doi.org/10.1109/83.777099.

Stewart, R., 1991, Exploration seismic tomography: SEG.

Williamson, P. R., and M. Worthington, 1993, Resolution limits in ray tomography due to wave behavior: Numerical experiments: Geophysics, 58, 727–735, https://doi.org/10.1190/1.1443457.